

Inhibitory receptors bind ANGPTLs and support blood stem cells and leukaemia development

Junke Zheng^{1,2*}, Masato Umikawa^{1,3*}, Changhao Cui^{1*}, Jiyuan Li¹, Xiaoli Chen¹, Chaozheng Zhang¹, HoangDinh Huynh¹, Xunlei Kang¹, Robert Silvány¹, Xuan Wan¹, Jingxiao Ye¹, Alberto Puig Cantó⁴, Shu-Hsia Chen⁵, Huan-You Wang⁶, E. Sally Ward⁴ & Cheng Cheng Zhang¹

How environmental cues regulate adult stem cell and cancer cell activity through surface receptors is poorly understood. Angiopoietin-like proteins (ANGPTLs), a family of seven secreted glycoproteins, are known to support the activity of haematopoietic stem cells (HSCs) *in vitro* and *in vivo*^{1–10}. ANGPTLs also have important roles in lipid metabolism, angiogenesis and inflammation, but were considered ‘orphan ligands’ because no receptors were identified^{3,11,12}. Here we show that the immune-inhibitory receptor human leukocyte immunoglobulin-like receptor B2 (LILRB2) and its mouse orthologue paired immunoglobulin-like receptor (PIRB) are receptors for several ANGPTLs. LILRB2 and PIRB are expressed on human and mouse HSCs, respectively, and the binding of ANGPTLs to these receptors supported *ex vivo* expansion of HSCs. In mouse transplantation acute myeloid leukaemia models, a deficiency in intracellular signalling of PIRB resulted in increased differentiation of leukaemia cells, revealing that PIRB supports leukaemia development. Our study indicates an unexpected functional significance of classical immune-inhibitory receptors in maintenance of stemness of normal adult stem cells and in support of cancer development.

We used multiple approaches, including expression cloning, to identify the receptor(s) for ANGPTLs. Human LILRB2, when ectopically expressed on Baf3 cells, enabled the cells to specifically bind glutathione *S*-transferase (GST)–ANGPTL5 as determined by flow cytometry (Fig. 1a). LILRB2 is a member of the immune-inhibitory B-type subfamily of LILR receptors¹³ and contains four immunoglobulin domains and three immunoreceptor tyrosine-based inhibitory motifs. Using flow cytometry analysis, we further demonstrated that LILRB2-overexpressing 293T cells demonstrated enhanced binding to several ANGPTLs, especially ANGPTL2 and GST–ANGPTL5 (Fig. 1b and Supplementary Fig. 1a, b). ANGPTL2 and GST–ANGPTL5 also bound to LILRB3- and LILRB5-overexpressing cells, although with a lower affinity than to LILRB2-expressing cells (Supplementary Table 1). In addition, ANGPTL1 and ANGPTL7 bound to 293T cells overexpressing LAIR1 (ref. 14). (Supplementary Table 1 and Supplementary Fig. 2). ANGPTLs did not bind to LILRAs, LILRB1 or LILRB4 (Supplementary Table 1).

Because ANGPTL2 and GST–ANGPTL5 bound to LILRB2-expressing cells better than other ANGPTLs, we further assessed the molecular interaction between ANGPTL2/ANGPTL5 and LILRB2.

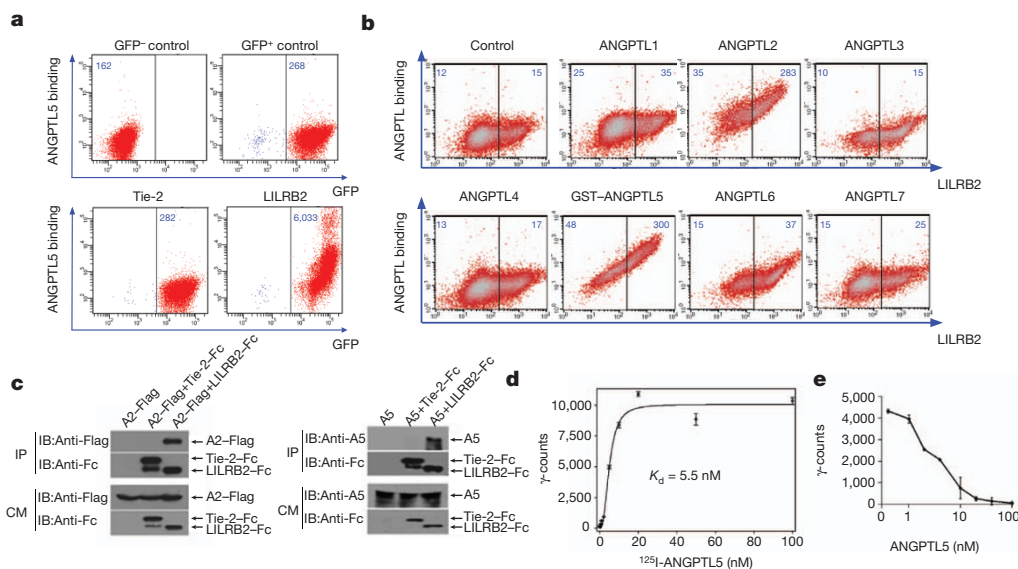


Figure 1 | Cell-surface LILRB2 binds to ANGPTLs. **a**, Flow cytometry analysis of GST–ANGPTL5–Flag binding to uninfected Baf3 cells or MSCV–GFP, MSCV–Tie-2–GFP- or MSCV–LILRB2–GFP-stably infected Baf3 cells. Mean fluorescence intensities are indicated. **b**, Flow cytometry analysis of indicated Flag-tagged ANGPTLs binding to LILRB2-transfected 293T cells.

c, ANGPTL2 and ANGPTL5 bound to the ECD of LILRB2 but not Tie-2 in conditioned medium (CM) of cotransfected 293T cells. **d**, **e**, Concentration-dependent specific (**d**) and competitive (**e**) ¹²⁵I–GST–ANGPTL5 binding to LILRB2 stably expressed Baf3 cells (*n* = 3). Error bars denote s.e.m. IB, immunoblotting.

¹Departments of Physiology and Developmental Biology, University of Texas Southwestern Medical Center, Dallas, Texas 75390, USA. ²Key Laboratory of Cell Differentiation and Apoptosis of Chinese Ministry of Education, Shanghai Jiao Tong University School of Medicine, Shanghai 200025, China. ³Department of Medical Biochemistry, University of the Ryukyus, Okinawa 903-0215, Japan. ⁴Department of Immunology, University of Texas Southwestern Medical Center, Dallas, Texas 75390, USA. ⁵Department of Oncological Sciences, Mount Sinai School of Medicine, New York, New York 10029-6574, USA. ⁶Department of Pathology, University of California San Diego, La Jolla, California 92093, USA.

*These authors contributed equally to this work.

Co-transfection of ANGPTL2 or ANGPTL5 with LILRB2 extracellular domain (ECD) fused to human IgG-Fc (LILRB2-Fc) into 293T cells followed by immunoprecipitation and western blot showed that both ANGPTL2 and ANGPTL5 interacted with the ECD of LILRB2, but not that of Tie-2 (Fig. 1c and Supplementary Fig. 1c). The direct interactions between ANGPTLs and LILRB2 were confirmed by *in vitro* coimmunoprecipitation, using purified ANGPTL2-Flag or GST-ANGPTL5 and LILRB2-Fc (Supplementary Fig. 1d) and by surface plasmon resonance (SPR; Supplementary Fig. 3). A liquid-phase binding assay with ^{125}I -labelled GST-ANGPTL5 demonstrated that the interaction between ANGPTL5 and cell-surface LILRB2 was specific and saturable, with half maximal saturation of the interaction as 5.5 ± 1.1 nM (Fig. 1d, e). Although untagged ANGPTLs bind to LILRB2, the type or the position of tagging could affect the binding (Supplementary Table 2).

Because several ANGPTLs support expansion of HSCs^{4–10}, we sought to determine whether ANGPTLs bound to LILRB2 or LAIR1 on primary human cord blood cells. Flow cytometry analysis showed that ANGPTL 1, 2, 5 and 7 all bound to LILRB2⁺ human cord blood cells, and that ANGPTL2 and GST-ANGPTL5 had higher affinities (Fig. 2a, Supplementary Fig. 4 and Supplementary Table 1). The binding of ANGPTL1 and ANGPTL7 to LAIR1⁺ human cord blood cells was relatively weak (Supplementary Fig. 5), and we therefore focused on studying the binding of ANGPTL2 and ANGPTL5 to LILRB2 in subsequent experiments.

We determined whether LILRB2 was expressed on human HSCs. Flow cytometry and quantitative (q)RT-PCR analyses showed that LILRB2 was expressed on the surface of 40–95% of human cord blood CD34⁺ CD38⁻ CD90⁺ cells (95% in the experiment shown in Fig. 2b and Supplementary Fig. 6); this population is enriched for HSCs.

GST-ANGPTL5 treatment induced increased phosphorylation of calcium/calmodulin-dependent protein kinase (CAMK)-2 and -4 in human cord blood mononuclear cells (Supplementary Fig. 7). It is of note that CAMK4 is required for maintenance of the potency of HSCs¹⁵. Suppression of LILRB2 expression with short hairpin RNAs effectively reduced ANGPTL binding (Supplementary Fig. 8). Importantly, the silencing of LILRB2 resulted in decreased repopulation of human cord blood HSCs as measured by reconstitution analysis in non-obese diabetic/severe combined immunodeficient (NOD/SCID) mice (1% repopulation from cultured knockdown cells compared to 15% repopulation from cultured normal cells in medium STFA5; Fig. 2c). Together, these data indicate that ANGPTL5 supports expansion of human cord blood HSCs¹ in a process at least partially mediated by the surface receptor LILRB2.

PIRB is the mouse membrane orthologue of human LILRBs^{16,17}. ANGPTL2, ANGPTL3 and GST-ANGPTL5 bound to PIRB as determined by flow cytometry (Fig. 3a and Supplementary Fig. 9) and coimmunoprecipitation (Fig. 3b and Supplementary Fig. 10). As with human cord blood HSCs, mouse HSCs were also enriched for PIRB expression (Fig. 3c and Supplementary Fig. 11).

To study the function of PIRB in mouse HSCs, we used PIRB-deficient (PIRBTM) mice¹⁸, in which four exons encoding the trans-membrane domain and part of the intracellular domain were deleted. PIRBTM cells freshly isolated from 3-week-old mice had significantly decreased CAMK4 phosphorylation, and binding of ANGPTL to PIRB induced phosphorylation of PIRB, recruitment of SHP-1 and SHP-2 (also known as PTPN6 and PTPN11, respectively) and CAMK4 activation (Supplementary Figs 12 and 13). These results suggest that certain ANGPTLs may be the ligands of PIRB that activate CAMK4 *in vivo*.

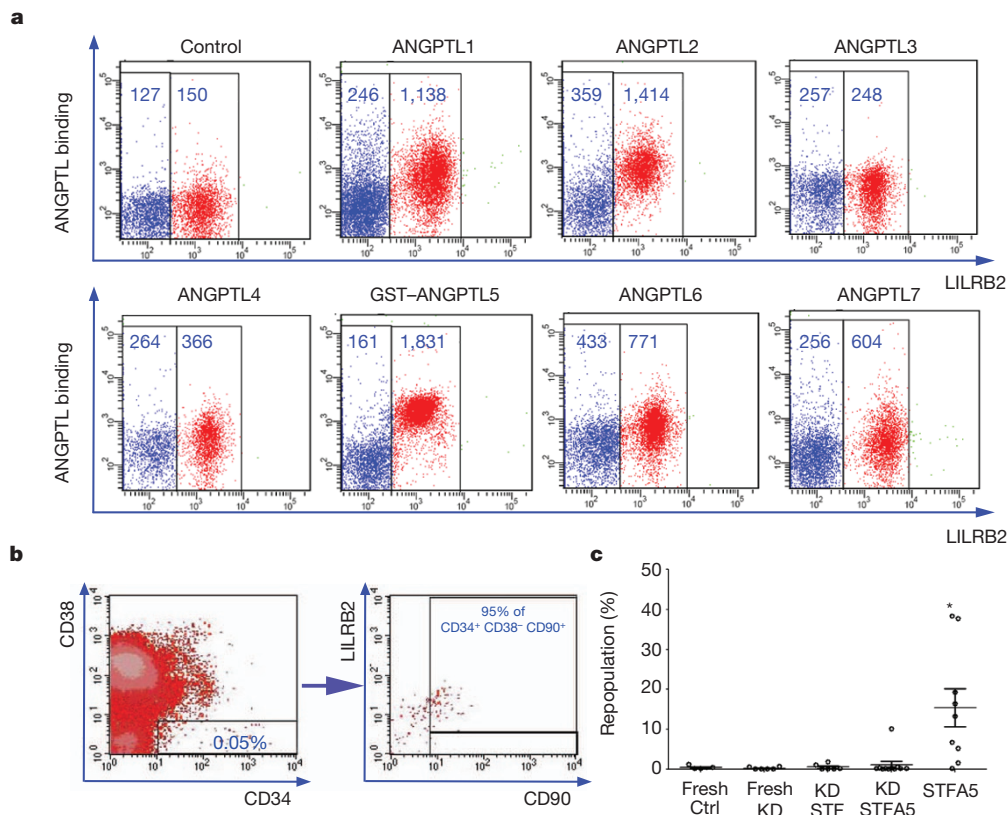


Figure 2 | LILRB2 mediates the effect of ANGPTL in supporting the repopulation of human cord blood HSCs. **a**, Flow cytometry analysis of indicated Flag-tagged ANGPTLs binding to LILRB2⁺ human cord blood mononuclear cells (FACSARIA). Mean fluorescence intensities are indicated. **b**, Representative flow cytometry plots for the co-staining of CD34, CD38, CD90 and LILRB2 in human cord blood mononuclear cells (FACS-Calibur).

c, Human cord blood CD34⁺ cells infected with LILRB2 shRNA-encoding virus (KD) or control (Ctrl) scramble shRNA virus were transplanted into sublethally irradiated NOD/SCID mice before or after culture for 10 days. SCF+TPO+Flt3L (STF) or STF+ANGPTL5 (STFA5) was used in the culture. Shown is the human donor repopulation after 2 months ($n = 5–11$). * $P < 0.05$. Error bars denote s.e.m.

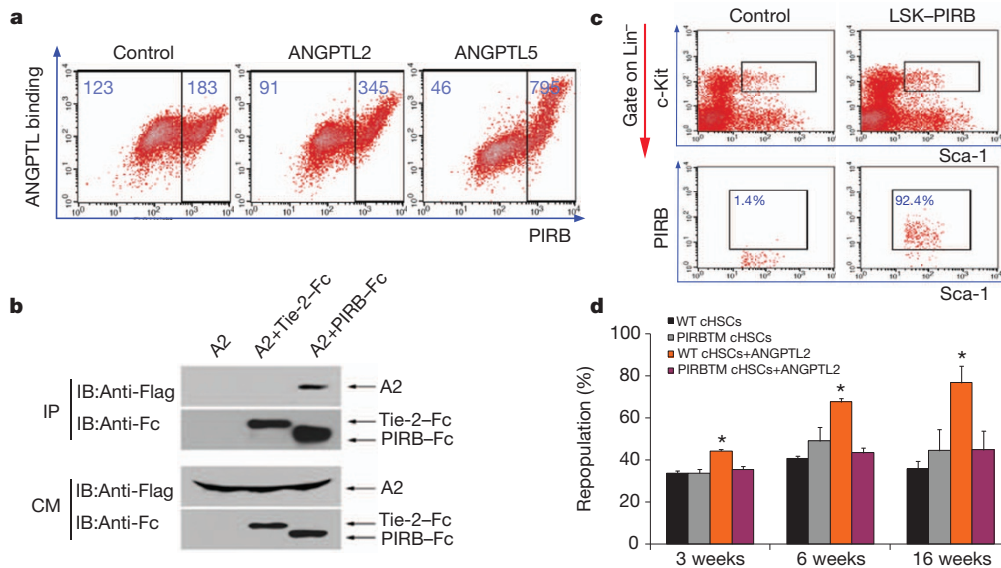


Figure 3 | ANGPTLs bind PIRB and support the repopulation of mouse HSCs. **a**, Flow cytometry analysis of Flag-ANGPTL2 or GST-ANGPTL5-Flag binding to PIRB-transfected 293T cells. **b**, ANGPTL2 binds to the ECD of PIRB but not Tie-2 in the conditioned medium (CM) of cotransfected 293T cells. **c**, PIRB is expressed on mouse bone marrow (BM) Lin⁻ Sca-1⁺ Kit⁺ (LSK)

Because SHP-2 and CAMK4 are required for the repopulation of HSCs^{15,19}, and the chemical inhibition of CAMK2, a homologue of CAMK4, induces differentiation and suppresses proliferation of myeloid leukaemia cells²⁰, we sought to determine whether PIRB was important for HSC activity. Although the adult PIRBTM mice have certain immune and neuronal defects, they are grossly normal in haematopoiesis^{16,18}. Interestingly, competitive repopulation showed that PIRBTM fetal liver HSCs had approximately 50% decreased repopulation activity (Supplementary Fig. 14). Moreover, although ANGPTL2 and ANGPTL5 had little effect on *ex vivo* expansion of adult PIRBTM HSCs, they supported *ex vivo* expansion of adult wild-type HSCs (Fig. 3d and Supplementary Fig. 14), as we previously demonstrated². Collectively, our results indicate that ANGPTLs bind human LILRB2 and mouse PIRB to support HSC repopulation.

On the basis of our *in silico* analysis of a pool of 9,004 samples described previously²¹, the level of LILRB2 messenger RNA is at least fourfold higher in the human acute monoblastic and monocytic leukaemia cells (M5 subtype of acute myeloid leukaemia (AML)) than in other AML cells (Supplementary Fig. 15). As human acute monoblastic and monocytic leukaemia cells are often associated with rearrangement of mixed-lineage leukaemia (MLL; a histone methyltransferase deemed a positive global regulator of gene transcription), we used a retroviral MLL-AF9 transplantation mouse model^{22,23} to further examine the role of PIRB in regulation of AML development. Wild-type or PIRBTM donor Lin⁻ cells infected by retroviral MLL-AF9-internal ribosome entry site (IRES)-yellow fluorescent protein (YFP) were used to induce AML as previously described^{22,23}. We examined PIRB expression in YFP⁺ Mac-1⁺ Kit⁺ cells that may be enriched for AML-initiating activity^{22,23}, and found that about 80% of YFP⁺ Mac-1⁺ Kit⁺ cells were PIRB⁺ (Fig. 4a). We next investigated whether PIRB was required for the induction of AML by MLL-AF9. Mice transplanted with MLL-AF9-transduced wild-type cells developed AML and died within approximately 5 weeks, whereas those transplanted with MLL-AF9-transduced PIRBTM cells were resistant to the induction of MLL-AF9 and developed AML much more slowly (Fig. 4b and Supplementary Fig. 16). The significantly delayed development of the PIRBTM leukaemia was correlated with about a 50% reduction in numbers of white blood cells in circulation and a much less severe infiltration of myeloid leukaemia cells into

the liver and spleen (Fig. 4c, d). Consistently, PIRB deficiency caused an approximately 50% reduction of YFP⁺ Mac-1⁺ Kit⁺ cells in both bone marrow and peripheral blood (Fig. 4d). There were more CD3⁺ or B220⁺ cells in mice that received MLL-AF9-transduced PIRBTM donor cells than in those given wild-type cells (Fig. 4d). These results demonstrate that PIRB-mediated signalling is associated with faster AML development and greater numbers of YFP⁺ Mac-1⁺ Kit⁺ AML cells *in vivo*.

We further assessed whether PIRB potentially regulates differentiation and self-renewal of AML cells. Colony-forming unit (c.f.u.) assays showed that extrinsic ANGPTL stimulation led to increased c.f.u. numbers in wild-type but not PIRBTM AML cells, again indicating that PIRB directly mediates the effects of ANGPTLs (Supplementary Fig. 16d). In addition, wild-type AML cells formed mostly compact colonies, whereas PIRBTM cells tended to form more diffuse ones (Fig. 4e). The formation of diffuse colonies indicates high differentiation potential²⁴. The inhibition of differentiation of AML cells by PIRB is in accordance with previous reports that PIRB inhibits differentiation of myeloid-derived suppressive cells²⁵ and osteoclasts²⁶, as well as our data showing that endogenous ANGPTLs inhibit differentiation and increase replating efficiency of haematopoietic progenitors (Supplementary Fig. 17). Moreover, PIRBTM primary colony-forming units were unable to form secondary colonies upon replating (Fig. 4f), indicating that PIRB supports self renewal of AML c.f.u. cells.

Finally, we analysed the molecular signalling triggered by the binding of ANGPTLs to PIRB in AML cells. PIRBTM AML cells had decreased phosphorylation of phosphatase SHP-2 (Supplementary Fig. 13d), which is known to be associated with LILRB receptors and is an oncogene that supports leukaemia development^{13,16,18,27}. ANGPTLs also stimulated SHP-2 phosphorylation (Supplementary Fig. 13d). Similar to untransformed PIRBTM cells, PIRBTM AML cells had decreased CAMK4 activation (data not shown). Furthermore, wild-type Mac-1⁺ Kit⁺ cells had much greater expression of leukaemia initiation/maintenance genes^{22,23}, but markedly decreased expression of myeloid-differentiation genes as determined by DNA microarray analyses (Fig. 4g). qRT-PCR confirmed the increased expression of several *HOXA* genes, *Meis1*, *Eya1*, *Myb* and *Mef2c* in wild-type Mac-1⁺ Kit⁺ cells than their PIRBTM counterparts (Supplementary Fig. 18); these genes are critical for initiation or maintenance of MLL-rearranged

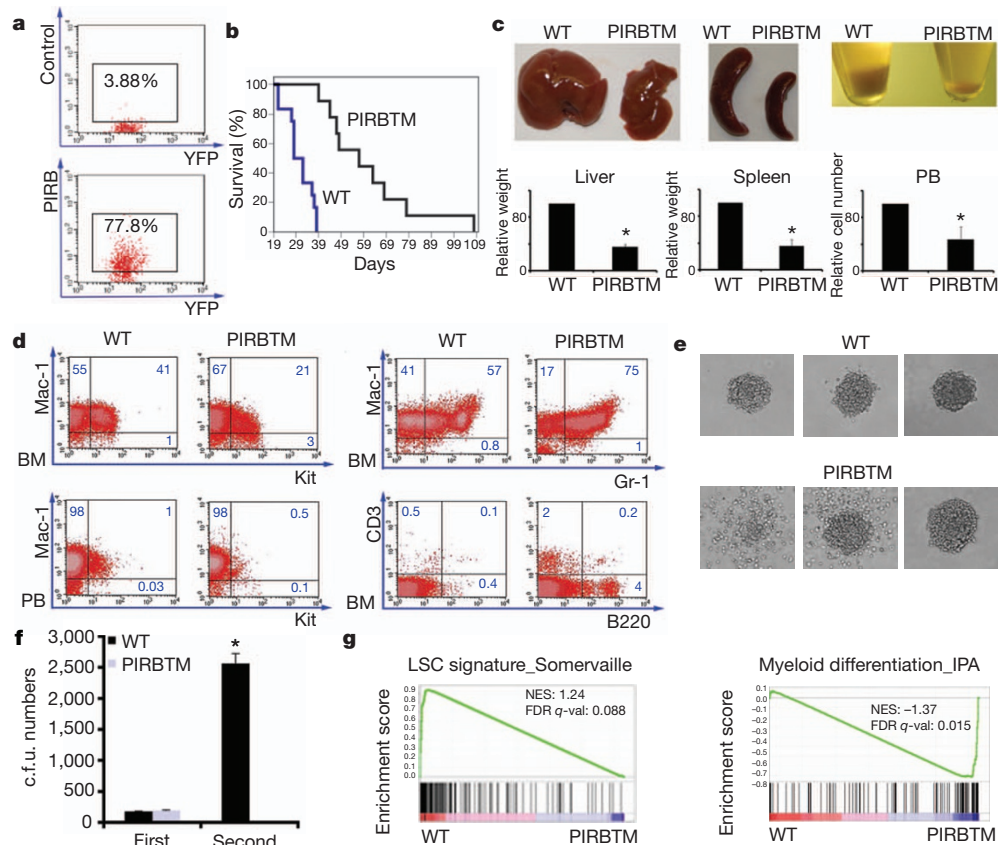


Figure 4 | PIRB suppresses differentiation and enhances development of MLL-AF9 AML. **a**, PIRB expression on YFP⁺ Mac-1⁺ Kit⁺ AML cells as determined by flow cytometry. **b**, Survival curve of mice receiving MLL-AF9-infected WT or PIRBTM haematopoietic progenitors ($n = 15$); $P < 0.05$. **c**, Comparison of the sizes of spleen, liver and numbers of peripheral blood (PB) cells of the mice transplanted with wild-type (WT) MLL-AF9 cells and PIRBTM MLL-AF9 cells at 28 days after transplantation ($n = 6$). **d**, Representative flow cytometry plots showing that PIRBTM AML mice have decreased Mac-1⁺ Kit⁺ cells and increased differentiated cells relative to mice transplanted with WT cells

AML (refs 22, 23). Similar to the MLL-AF9 model, the deficiency of PIRB in the AML1-ETO9a leukaemia model led to decreased numbers of leukaemia progenitors and increased numbers of differentiated cells (Supplementary Fig. 19). Collectively, these results indicate that the binding of ANGPTLs to PIRB promotes leukaemia development, probably through inhibiting differentiation of AML cells.

LILRB2 and PIRB are known to bind to other ligands, including various MHC class I molecules²⁸ and myelin inhibitors¹⁷. It will be important to investigate the *in vivo* context in which these different ligands bind LILRB and induce signalling. As ANGPTLs can be abundantly expressed by many types of cells, including those from endocrine organs¹¹ and potential bone marrow niche (endothelium and adipocytes^{9,11}), and can be induced by hypoxia¹¹, these secreted factors may have important direct and indirect effects on the activities of HSCs and leukaemia stem cells *in vivo*. Although the LILRB/PIRB receptors were reported to suppress activation of differentiated immune cells and inhibit neurite outgrowth of neural cells^{16,17}, they support HSC repopulation and inhibit differentiation of AML cells. This result suggests the importance of these ‘inhibitory receptors’ in maintenance of stemness of normal stem cells and support of leukaemia development. In contrast to the ‘stimulatory receptors’ such as interferon receptors or Toll-like receptors that activate and induce differentiation of HSCs upon inflammation²⁹, LILRB2 and PIRB may function as sensors of inflammation through binding to the inflammatory ANGPTLs¹² and protecting HSCs from excessive activation and exhaustion. Adult stem cells and cancer cells probably require

both stimulatory receptors and inhibitory receptors to maintain the balance of their cell fates.

at 28 days after transplantation. **e**, Comparison of colony-forming activity of WT and PIRBTM MLL-AF9⁺ bone marrow cells. Shown is typical morphology of WT and PIRBTM colony-forming units. **f**, PIRBTM MLL-AF9 bone marrow cells have markedly decreased colony-forming ability in second replating ($n = 3$). **g**, Gene set enrichment analysis plots evaluating changes in leukaemia initiation/maintenance and myeloid-differentiation gene signatures upon PIRB signalling depletion in WT or PIRBTM MLL-AF9 Mac-1⁺ Kit⁺ AML cells. $*P < 0.05$. Error bars denote s.e.m. FDR q -val, false-discovery rate q -value; NES, normalized enrichment score.

both stimulatory receptors and inhibitory receptors to maintain the balance of their cell fates.

METHODS SUMMARY

Plasmid cytomegalovirus (CMV)-Kozak human Angiotensin-converting enzyme 1 and ANGPTL 1, 2, 3, 4, 6 and 7 with Flag tags at the carboxy terminus were used for transfection. ANGPTL2-Flag was purified using M2 resin. Purified GST-ANGPTL5 was purchased from Abnova. Bacterially expressed Flag-ANGPTL2 (with Flag at the amino terminus) and ANGPTL2-Flag (with Flag at the C terminus) were constructed in pET-26b(+) vector, and GST-ANGPTLs-Flag in pGEX vector, and expressed and purified from bacteria. Murine stem cell virus (MSCV)-LILRB2-IRES-green fluorescent protein (GFP) or control retrovirus-infected Baf3 cells, CMV-driven LILRA-, LILRB-, PIRB-, or LAIR1-transfected 293T cells, or human mononuclear cord blood cells were used in binding assays. See the Methods for detailed experimental methods for flow cytometry, coimmunoprecipitation, SPR, liquid-phase binding, culture, transplantation, c.f.u. and gene set enrichment analysis (GSEA). Mice were maintained at the University of Texas Southwestern Medical Center animal facility. All animal experiments were performed with the approval of University of Texas Southwestern Committee on Animal Care.

Full Methods and any associated references are available in the online version of the paper at www.nature.com/nature.

Received 15 July 2011; accepted 29 March 2012.

- Zhang, C. C., Kaba, M., Iizuka, S., Huynh, H. & Lodish, H. F. Angiotensin-like 5 and IGFBP2 stimulate *ex vivo* expansion of human cord blood hematopoietic stem cells as assayed by NOD/SCID transplantation. *Blood* **111**, 3415–3423 (2008).

2. Zhang, C. C. *et al.* Angiotensin-like proteins stimulate *ex vivo* expansion of hematopoietic stem cells. *Nature Med.* **12**, 240–245 (2006).
3. Zhang, C. C. & Lodish, H. F. Cytokines regulating hematopoietic stem cell function. *Curr. Opin. Hematol.* **15**, 307–311 (2008).
4. Huynh, H. *et al.* IGF1 secreted by a tumorigenic cell line supports *ex vivo* expansion of mouse hematopoietic stem cells. *Stem Cells* **26**, 1628–1635 (2008).
5. Chou, S. & Lodish, H. F. Fetal liver hepatic progenitors are supportive stromal cells for hematopoietic stem cells. *Proc. Natl Acad. Sci. USA* **107**, 7799–7804 (2010).
6. Lin, M. & Zon, L. I. Genetic analyses in zebrafish reveal that angiotensin-like proteins 1 and 2 are required for HSC development during embryogenesis. *Am. Soc. Hematol. 50th Ann. Meeting Abstract* 729 186 (2008).
7. Khoury, M. *et al.* Mesenchymal stem cells secreting angiotensin-like-5 support efficient expansion of human hematopoietic stem cells without compromising their repopulating potential. *Stem Cells Dev.* **20**, 1371–1381 (2011).
8. Drake, A. C. *et al.* Human CD34⁺ CD133⁺ hematopoietic stem cells cultured with growth factors including Angptl5 efficiently engraft adult NOD-SCID Il2 γ ^{-/-} (NSG) mice. *PLoS ONE* **6**, e18382 (2011).
9. Zheng, J., Huynh, H., Umikawa, M., Silvano, R. & Zhang, C. C. Angiotensin-like protein 3 supports the activity of hematopoietic stem cells in the bone marrow niche. *Blood* **117**, 470–479 (2011).
10. Zheng, J. *et al.* *Ex vivo* expanded hematopoietic stem cells overcome the MHC barrier in allogeneic transplantation. *Cell Stem Cell* **9**, 119–130 (2011).
11. Hato, T., Tabata, M. & Oike, Y. The role of angiotensin-like proteins in angiogenesis and metabolism. *Trends Cardiovasc. Med.* **18**, 6–14 (2008).
12. Tabata, M. *et al.* Angiotensin-like protein 2 promotes chronic adipose tissue inflammation and obesity-related systemic insulin resistance. *Cell Metab.* **10**, 178–188 (2009).
13. Barrow, A. D. & Trowsdale, J. The extended human leukocyte receptor complex: diverse ways of modulating immune responses. *Immunol. Rev.* **224**, 98–123 (2008).
14. Meyaard, L. LAIR and collagens in immune regulation. *Immunol. Lett.* **128**, 26–28 (2010).
15. Kitsos, C. M. *et al.* Calmodulin-dependent protein kinase IV regulates hematopoietic stem cell maintenance. *J. Biol. Chem.* **280**, 33101–33108 (2005).
16. Takai, T., Nakamura, A. & Endo, S. Role of PIR-B in autoimmune glomerulonephritis. *J. Biomed. Biotechnol.* **2011**, 275302 (2011).
17. Atwal, J. K. *et al.* PirB is a functional receptor for myelin inhibitors of axonal regeneration. *Science* **322**, 967–970 (2008).
18. Syken, J., Grandpre, T., Kanold, P. O. & Shatz, C. J. PirB restricts ocular-dominance plasticity in visual cortex. *Science* **313**, 1795–1800 (2006).
19. Chan, R. J. *et al.* Shp-2 heterozygous hematopoietic stem cells have deficient repopulating ability due to diminished self-renewal. *Exp. Hematol.* **34**, 1229–1238 (2006).
20. Si, J. & Collins, S. J. Activated Ca²⁺/calmodulin-dependent protein kinase II γ is a critical regulator of myeloid leukemia cell proliferation. *Cancer Res.* **68**, 3733–3742 (2008).
21. Lusk, M. *et al.* A global map of human gene expression. *Nature Biotechnol.* **28**, 322–324 (2010).
22. Krivtsov, A. V. *et al.* Transformation from committed progenitor to leukaemia stem cell initiated by MLL-*AF9*. *Nature* **442**, 818–822 (2006).
23. Somervaille, T. C. & Cleary, M. L. Identification and characterization of leukemia stem cells in murine MLL-*AF9* acute myeloid leukemia. *Cancer Cell* **10**, 257–268 (2006).
24. Lavau, C., Szilvassy, S. J., Slany, R. & Cleary, M. L. Immortalization and leukemic transformation of a myelomonocytic precursor by retrovirally transduced HRX-ENL. *EMBO J.* **16**, 4226–4237 (1997).
25. Ma, G. *et al.* Paired immunoglobulin-like receptor-B regulates the suppressive function and fate of myeloid-derived suppressor cells. *Immunity* **34**, 385–395 (2011).
26. Mori, Y. *et al.* Inhibitory immunoglobulin-like receptors LILRB and PIR-B negatively regulate osteoclast development. *J. Immunol.* **181**, 4742–4751 (2008).
27. Chan, R. J. & Feng, G. S. PTPN11 is the first identified proto-oncogene that encodes a tyrosine phosphatase. *Blood* **109**, 862–867 (2007).
28. Shiroishi, M. *et al.* Human inhibitory receptors Ig-like transcript 2 (ILT2) and ILT4 compete with CD8 for MHC class I binding and bind preferentially to HLA-G. *Proc. Natl Acad. Sci. USA* **100**, 8856–8861 (2003).
29. Baldrige, M. T., King, K. Y. & Goodell, M. A. Inflammatory signals regulate hematopoietic stem cells. *Trends Immunol.* **32**, 57–65 (2011).

Supplementary Information is linked to the online version of the paper at www.nature.com/nature.

Acknowledgements We thank S. Armstrong for the MSCV-MLL-*AF9*-IRES-YFP construct, H. Hobbs for the CMV-ANGPTL6-Flag plasmid, T. Takai for providing the PIRB knockout mice to S.-H.C., X.-J. Xie for binding analysis, and UTSW Genomics and Microarray Core facility for DNA array experiments. S.-H.C. thanks support from NIH. C.C.Z. was supported by NIH grant K01 CA 120099, American Society of Hematology Junior Faculty Award, March of Dimes Basil O'Connor Scholar Award, DOD PR093256, CPRIT RP100402, and the Gabrielle's Angel Foundation.

Author Contributions J.Z., M.U., C.C. and C.C.Z. were responsible for the study design, identification of receptors, binding, signalling and functional assays, data analysis and writing of the manuscript. J.L., X.C., C.Z., H.H., X.K., R.S. and X.W. were responsible for binding and signalling assays and data analysis. J.Y. and S.-H.C. carried out the ligand-binding assays, H.-Y.W. carried out AML characterization, and A.P.C. and E.S.W. carried out the SPR assay and data analysis.

Author Information DNA microarray data are available for download from the GEO under accession number GSE36329. Reprints and permissions information is available at www.nature.com/reprints. The authors declare no competing financial interests. Readers are welcome to comment on the online version of this article at www.nature.com/nature. Correspondence and requests for materials should be addressed to C.C.Z. (Alec.Zhang@UTsouthwestern.edu).

METHODS

Mice. C57BL/6 CD45.2 and CD45.1 mice, or NOD/SCID mice, were purchased from the University of Texas Southwestern Medical Center animal breeding core facility. The PIRBTM mice¹⁸ were obtained from the MMRRC. The PIRB knockout mice²⁰ were a gift from T. Takai. Mice were maintained at the University of Texas Southwestern Medical Center animal facility. All animal experiments were performed with the approval of the University of Texas Southwestern Committee on Animal Care.

Plasmids and proteins. Plasmid CMV-Kozak human Ang1 and ANGPTLs 1, 2, 3, 4, 6 and 7 with Flag tags at the C terminus were transfected into 293T cells using Lipofectamine 2000, and the conditioned medium at 48 h was collected and different ANGPTL proteins were adjusted to the same level for flow cytometry-based binding experiments. ANGPTL2-Flag was purified using M2 resin. Purified GST-ANGPTL5 was purchased from Abnova. Bacterially expressed Flag-ANGPTL2 and ANGPTL2-Flag were constructed in pET-26b(+) vectors, and GST-ANGPTLs-Flag in pGEX vectors, and expressed and purified from bacteria. MSCV-LILRB2-IRES-GFP- or control retrovirus-infected Baf3 cells, or CMV-driven LILRA-, LILRB-, PIRB- or LAIR1-transfected 293T cells collected at 48 h, or mononuclear human cord blood cells were incubated with Fc block and equal amounts of different Flag-tagged ANGPTLs at 4 °C for 60 min, followed by staining with anti-Flag-allophycocyanin (APC) and propidium iodide. Anti-LILRB2-phycoerythrin (PE) was used as indicated. Cells were analysed using either a FACSCalibur or FACSAria instrument (Becton, Dickinson).

Antibodies and shRNAs. Flow cytometry antibodies anti-CD34-fluorescein isothiocyanate (FITC), anti-CD38-PE, anti-CD90-PE/Cy5.5, biotinylated lineage cocktail, anti-Kit-APC, anti-Sca-1-FITC, anti-Mac-1-APC, anti-Gr-1-PE, anti-CD3-APC and anti-B220-PE were purchased from BD Biosciences and used as described^{4,9,10,31}. The manufacturers and catalogue numbers for other antibodies are as follows: anti-LILRB1, Biologend (33707); anti-LILRB2, eBioscience (12-5149); anti-LILRB3, eBioscience (12-5159); anti-LILRB4, eBioscience (12-5139); anti-LILRB5, R&D Systems (AF3065); anti-PIRB-PE, R&D Systems (FAB2754P); anti-human LAIR1-PE, BD Pharmingen (550811); anti-mouse LAIR1-PE, eBioscience (12-3051); anti-Flag-APC, Prozyme (PJ255); anti-pCAMK2, Abcam (ab32678); anti-pCAMK4, Santa Cruz (sc-28443-R); anti-CAMK2, Cell Signaling (4436); anti-CAMK4, Cell Signaling (4032); anti-ANGPTL5, Abcam (ab57240); anti-PIRB, BD Pharmingen (550348) for coimmunoprecipitation of PIRB; anti-SHP-2, Cell Signaling (33975) for coimmunoprecipitation of SHP-2; and anti-Fc, Jackson ImmunoResearch (109-036-098). Combinations of multiple lentivirus-expressed shRNAs for inhibition of LILRB2 (hairpin sequences: TGCTGTTGACAGTGAGCGCCAGCTTGACCCTCAGACGGAATAGTGAAGCCACAGATGTATTCCGTCTGAGGGTCAAGCTGTTGCCTACTGCCTCGGA and TGCTGTTGACAGTGAGCGCAGCAGACCAGAGCTTGTGAAGAATAGTGAAGCCACAGACAGATGTATTCTTCAAGCTCTGGTCGTATGCCTACTGCCTCGGA); ANGPTL1 (TGCTGTTGACAGTGAGCGCCTCGTGTACTCAACTTATATAGTGAAGCCACAGATGTATATAGAGTTGAGTAAACACGAGATGCTACTGCCTCGGA, TGCTGTTGACAGTGAGCGAAGAGACTCGCCAATTTAAATAGTGAAGCCACAGATGTATTTAAATTGGCGAGTGTCTTCTGCCTACTGCCTCGGA and TGCTGTTGACAGTGAGCGCAGCAGACAGTGTATAAGTGAAGCCACAGATGTAATAGTGTCCAGCTCCATCTGATGCCTACTGCCTCGGA); ANGPTL3 (TGCTGTTGACAGTGAGCGACTCAGAAGGACTAGTATTCAATAGTGAAGCCACAGATGTATTGAATACTAGTCTCTGAGCTGCCTACTGCCTCGGA, TGCTGTTGACAGTGAGCGCAGCAGCAGTGTATTTTATTGACTATGCTGTTGCCTACTGCCTCGGA and TGCTGTTGACAGTGAGCGATACATATAAACTACAAGTCAATACTGGAAGCCACAGATGTATTGACTTGTAGTTTATAGTGTAGTGCCTACTGCCTCGGA); ANGPTL4 (TGCTGTTGACAGTGAGCGCAGCAGTGTATTGCAATAAATAAGTGAAGCCACAGATGTATTTTATTGACTATGCTGTTGCCTACTGCCTCGGA and TGCTGTTGACAGTGAGCGATACATATAAACTACAAGTCAATACTGGAAGCCACAGATGTATAAGCTTCTGCCGCTGCTGTTGCTACTGCCTCGGA and TGCTGTTGACAGTGAGCGCAGTGTAGTGTAGTGCCTACTGCCTCGGA); ANGPTL5 (TGCTGTTGACAGTGAGCGATAGAAGATGGATCTAATGCAATAGTGAAGCCACAGATGTATTGCAATTAGATCCATCTTACTGCCTACTGCCTCGGA, TGCTGTTGACAGTGAGCGAATGGTTTATGACTGATATAGTGAAGCCACAGATGTATATCAGTGAATCTAAACCATGTGCCTACTGCCTCGGA and TGCTGTTGACA

GTGAGCGATACGGACTCTTCAGTAGTAAATAGTGAAGCCACAGATGTA TTAAGTACTGAAGAGTCCGTAGTGCCTACTGCCTCGGA); ANGPTL6 (TGCTGTTGACAGTGAGCGCCACTACCTGGCAGCACTATAAATAGTGAAGCCACAGATGTATTAGTGTGCTGCCAGGTAGTGTGCTACTGCCTCGGA, TGCTGTTGACAGTGAGCGAGAGGCAAGATGGTTCAGTCAATAGTGAA GCCACAGATGTATTGACTGAACCATCTTGCTCCTGCCTACTGCCTCGGA and TGCTGTTGACAGTGAGCGACCCAGCAGAGACCCAGCAGCAGATA GTGAAGCCACAGATGTATCTGGGTCTGGTCTCTCTGGGGTGCCTACTG CCTCGGA); and ANGPTL7 (TGCTGTTGACAGTGAGCGCCCGGACTGG AAGCAGTACAATAGTGAAGCCACAGATGTATTGTACTGCTTCCAGTC CCGGTGCTACTGCCTCGGA, TGCTGTTGACAGTGAGCGCCCGCATC CTGGGAGTGTATAAATAGTGAAGCCACAGATGTATTATACACTCCAGATGTCGGTTCCTACTGCCTCGGA and TGCTGTTGACAGTGAGCGCGG ACTGAGAAACAGCCTATAAATAGTGAAGCCACAGATGTATTATAGGCTG TTTCTCAGTCTTGCCTACTGCCTCGGA) were purchased from Open Biosystems and used for knockdown experiments. The specificity of LILRB2 monoclonal antibody is confirmed by comparison of binding to all tested LILRA/Bs on transfected 293T cells. The specificities of other anti-LILRBs, anti-PIRB and anti-LAIR1 were confirmed by staining the respective complementary DNA-overexpressed 293T cells.

Coimmunoprecipitation. For *in vivo* coimmunoprecipitation, 293 cells were transiently co-transfected with plasmids encoding LILRB2-ECD-Fc, PIRB-ECD-Fc, or Tie-2-ECD-Fc and Flag-tagged ANGPTL2 or untagged ANGPTL5. Protein A beads were added to conditioned medium collected at 48 h after transfection, and proteins were detected by anti-Flag or anti-ANGPTL5 by western blot. For *in vitro* coimmunoprecipitation, purified ANGPTL2-Flag or GST-ANGPTL5 was incubated with purified LILRB2-ECD-Fc or Tie-2-ECD-Fc in PBS with 0.1% BSA and 0.1% NP-40 for 2 h followed by immunoprecipitation with protein A beads and western blotting.

Liquid-phase binding assay. Specific binding of radiolabelled GST-ANGPTL5 to Baf3 stably infected with MSCV-LILRB2-IRES-GFP (as LILRB2-Baf3 cells) was performed in a similar manner to before³². In brief, 6×10^6 LILRB2-Baf3 cells were incubated with ¹²⁵I-GST-ANGPTL5 (0.1–100 nM) in 200 μ l PBS/1% BSA for 3 h at 25 °C. Nonspecific binding on normal Baf3 cells was subtracted. In competition assay, 2.5×10^6 LILRB2-Baf3 or Baf3 cells were incubated with unlabelled GST-ANGPTL5 (0.1–100 nM) in 200 μ l PBS/1% BSA for 1 h at 25 °C, followed by addition of 5 nM of ¹²⁵I-GST-ANGPTL5 and incubation for 4 h. After incubation, the cells were washed twice by centrifugation, resuspended in ice-cold PBS with 1% BSA and then measured in a scintillation counter.

Cell culture and infection. Baf3 cells were grown in RPMI medium 1640 with 10% FBS and 10% Wehi conditioned cell medium. Human embryonic kidney 293T cells were grown in DMEM with 10% FBS.

For mouse HSC culture, indicated numbers of bone marrow Lin⁻Sca-1⁺Kit⁺CD34⁻Flk-2⁻ cells or fetal liver Lin⁻Sca-1⁺Kit⁺ cells isolated from 8–10-week-old C57BL/6 CD45.2 mice were plated in one well of a U-bottom 96-well plate (Corning) with 200 μ l of the indicated medium, essentially as we described previously^{4,9}. Cells were cultured at 37 °C in 5% CO₂ and indicated levels of O₂. For the purpose of competitive transplantation, we pooled cells from 12 culture wells and mixed them with competitor/supportive cells before the indicated numbers of cells were transplanted into each mouse. For western blotting, 3-week-old mouse spleen cells were cultured overnight in DME supplemented with 0.1% BSA, followed by treatment with indicated amount of ANGPTLs. Human mononuclear cord blood cells were cultured in DME containing 10% FBS overnight followed by starvation in serum-free DME for 4 h before ANGPTL stimulation.

The infection of Lin⁻ cells by MSCV-MLL-AF9-IRES-YFP and MSCV-AML1-ETO9a-IRES-GFP was performed after procedures described in refs 22,23 and 33, respectively. In brief, we incubated Lin⁻ cells overnight in medium with 10% FBS, 20 ng ml⁻¹ SCF, 20 ng ml⁻¹ IL-3 and 10 ng ml⁻¹ IL-6, followed by spin infection with retroviral supernatant in the presence of 4 μ g ml⁻¹ polybrene. Infected cells (300,000) were transplanted into lethally irradiated (1,000 rad) C57BL/6 mice by retro-orbital injection.

For human cell culture, fresh and cryopreserved human cord blood cells were obtained from University of Texas Southwestern Parkland Hospital through approved IRB protocol 042008-033. CD34⁺ cells were isolated by AutoMACS and grown essentially as we described^{14,10}. CD133⁺ cells were purchased from AllCell. Lentiviral infection by shRNAs for LILRB2 or ANGPTLs was performed as recommended by Open Biosystems.

Flow cytometry and reconstitution analysis. Donor mouse bone marrow cells were isolated from 8–10-week-old C57BL/6 CD45.2 mice. Bone marrow Lin⁻Sca-1⁺Kit⁺CD34⁻Flk-2⁻ cells were isolated by staining with a biotinylated lineage cocktail (anti-CD3, anti-CD5, anti-B220, anti-Mac-1, anti-Gr-1, anti-Ter119 and anti-7-4; Stem Cell Technologies) followed by streptavidin-PE/Cy5.5, anti-Sca-1-FITC, anti-Kit-APC, anti-CD34-PE, and anti-Flk-2-PE. The indicated numbers of mouse CD45.2 donor cells were mixed with 1×10^5 freshly isolated CD45.1

competitor bone marrow cells, and the mixture injected intravenously through the retro-orbital route into each of a group of 6–9-week-old CD45.1 mice previously irradiated with a total dose of 10 Gy. To measure reconstitution of transplanted mice, peripheral blood was collected at the indicated times post-transplant and CD45.1⁺ and CD45.2⁺ cells in lymphoid and myeloid compartments were measured as we described^{4,9,10}. The analyses of Mac-1, Kit, Gr-1, CD3 and B220 populations in AML blood or bone marrow were performed by using anti-Mac-1-APC, anti-Kit-PE, anti-Gr-1-PE, anti-CD3-APC and anti-B220-PE.

Uncultured or cultured progenies of human cells were pooled together and the indicated portions were injected intravenously through the retro-orbital route into sub-lethally irradiated (250 rad) 6–8-week-old NOD/SCID mice. 8 weeks after transplantation, bone marrow nucleated cells from transplanted animals were analysed by flow cytometry for the presence of human cells as we described^{1,10}.

c.f.u. assays. 2,000 YFP⁺ Mac-1⁺ Kit⁺ bone marrow cells from AML mice were plated in methylcellulose (M3534; Stem Cell Technologies) for c.f.u.–granulocyte macrophage assays, according to the manufacturer's protocols and our previously published protocol³⁴. After 7 days, 2,000 cells from three dishes initially plated were used for secondary replating.

Surface plasmon resonance. Biacore 2000 and CM5 chips were used to analyse binding of purified ANGPTLs to the LILRB2 ECD fused to Fc, using a method similar to that previously described³⁵. Recombinant protein A (Pierce) was pre-immobilized in two flow cells (~2,000 response units) using the amine-coupling kit from GE Healthcare. LILRB2–Fc was injected into one of the flow cells to be captured by the protein A to reach ~300 response units. GST–ANGPTL5 was injected over the immobilized LILRB2 in HBS–EP (GE Healthcare) containing 0.01 M HEPES (pH 7.4), 0.15 M NaCl and 0.005% polysorbate 20. Each binding sensorgram from the sample flow cell, containing a captured LILRB2–Fc, was corrected for the protein A-coupled cell control. After each injection of an antigen solution, which induced the binding reaction, and the dissociation period during which the running buffer was infused, the protein A surface was regenerated by the

injection of the regeneration solution containing 10 mM Na₃PO₄ (pH 2.5) and 500 mM NaCl. All captured LILRB2–Fc, with and without ANGPTL5 bound, was completely removed, and another cycle begun. All measurements were performed at 25 °C with a flow rate of 30 µl min⁻¹.

GSEA. GSEA³⁶ was performed using GSEA v2.0 software (<http://www.broadinstitute.org/gsea/index.jsp>) with 1,000 phenotype permutations, and normalized enrichment score and false-discovery rate *q*-value were calculated. Leukaemia-stem-cell and macrophage-development gene sets were obtained from the indicated publication³⁷.

Statistics. A two-tailed Student's *t*-test was performed to evaluate the significance between experimental groups, unless otherwise indicated. The survival rates of the two groups were analysed using a log-rank test.

30. Ujike, A. *et al.* Impaired dendritic cell maturation and increased T_H2 responses in PIR-B(−/−) mice. *Nature Immunol.* **3**, 542–548 (2002).
31. Simsek, T. *et al.* The distinct metabolic profile of hematopoietic stem cells reflects their location in a hypoxic niche. *Cell Stem Cell* **7**, 380–390 (2010).
32. Zhang, C. C., Krieg, S. & Shapiro, D. J. HMG-1 stimulates estrogen response element binding by estrogen receptor from stably transfected HeLa cells. *Mol. Endocrinol.* **13**, 632–643 (1999).
33. Yan, M. *et al.* A previously unidentified alternatively spliced isoform of t(8;21) transcript promotes leukemogenesis. *Nature Med.* **12**, 945–949 (2006).
34. Zhang, C. C., Steele, A. D., Lindquist, S. & Lodish, H. F. Prion protein is expressed on long-term repopulating hematopoietic stem cells and is important for their self-renewal. *Proc. Natl Acad. Sci. USA* **103**, 2184–2189 (2006).
35. Luo, Y., Lu, Z., Raso, S. W., Entrican, C. & Tangarone, B. Dimers and multimers of monoclonal IgG1 exhibit higher *in vitro* binding affinities to Fcγ receptors. *MAbs* **1**, 491–504 (2009).
36. Subramanian, A. *et al.* Gene set enrichment analysis: a knowledge-based approach for interpreting genome-wide expression profiles. *Proc. Natl Acad. Sci. USA* **102**, 15545–15550 (2005).
37. Zuber, J. *et al.* RNAi screen identifies Brd4 as a therapeutic target in acute myeloid leukaemia. *Nature* **478**, 524–528 (2011).

CORRIGENDUM

doi:10.1038/nature11268

Corrigendum: Inhibitory receptors bind ANGPTLs and support blood stem cells and leukaemia development

Junke Zheng, Masato Umikawa, Changhao Cui, Jiyuan Li,
Xiaoli Chen, Chaozheng Zhang, HoangDinh Huynh,
Xunlei Kang, Robert Silvany, Xuan Wan, Jingxiao Ye,
Alberto Puig Cantó, Shu-Hsia Chen, Huan-You Wang,
E. Sally Ward & Cheng Cheng Zhang

Nature **485**, 656–660 (2012); doi:10.1038/nature11095

The surname of author HoangDinh Huynh was inadvertently misspelled as Hyunh. This has been corrected online in the PDF and HTML of the original paper.